Use of sap flow measurements to validate stomatal functions for mature beech (*Fagus sylvatica*) in view of ozone uptake calculations

Sabine Braun[1)], Christian Schindler[2)] and Sebastian Leuzinger[3)],

[1)] Institute for Applied Plant Biology, Sangrubenstrasse 25, CH-4124 Schönenbuch, Switzerland

[2)] Swiss Tropical and Public Health Institute, University of Basel, Socinstrasse 57, CH-4051 Basel, Switzerland

[3)] Forest Ecology, Institute of Terrestrial Ecosystems, ETH Zurich, Universitätsstr. 16, 8092 Zürich, Switzerland

Abstract

For a quantitative estimate of the ozone effect on vegetation reliable models for ozone uptake through the stomata are needed. Because of the analogy of ozone uptake and transpiration it is possible to utilize measurements of water loss such as sap flow for quantification of ozone uptake. This technique was applied in three beech (*Fagus sylvatica*) stands in Switzerland. A canopy conductance was calculated from sap flow velocity and normalized to values between 0 and 1. It represents mainly stomatal conductance as the boundary layer resistance in forests is usually small. Based on this relative conductance, stomatal functions to describe the dependence on light, temperature, vapour pressure deficit and soil moisture were derived using multivariate nonlinear regression. These functions were validated by comparison with conductance values directly estimated from sap flow. The results corroborate the current flux parameterization for beech used in the DO_3SE model.

Capsule

A method was developed to derive stomatal functions and ozone uptake calculation from sap flow.

Keywords

Ozone uptake; sap flow; stomatal conductance; Fagus sylvatica, DO_3SE

Introduction

Ozone is recognized as a threat to forests (Skärby et al., 1998; Fuhrer et al., 1997). The effects include growth reduction (Reich, 1987; Karlsson et al., 2004; Braun et al., 2007), visible injury (Günthardt-Goerg et al., 1991), inhibition of carbon allocation (Wellburn and Wellburn, 1994; Samuelson and Kelly, 1996; McLaughlin and Kohut, 1992), impairment of stomatal function (Pearson and Mansfield, 1993; Maier-Maercker and Koch, 1991) and biotic interactions (Braun and Flückiger, 1989). Its significance is expected to increase in the future (Fowler et al., 1999), and it may decrease carbon sequestration or offset possible enhancements in net primary production by increased CO_2 concentrations (Sitch et al., 2007; Van Dingenen et al., 2009). To estimate ozone risk, dose-response relationships for forest trees have first been established using a quantification based on concentration measurements outside the trees (accumulated ozone over the threshold 40 ppb for daylight hours; AOT40) (Kärenlampi and Skärby, 1996; Fuhrer and Achermann, 1999). An external concentration is, however, unsatisfactory because only ozone taken up via stomata is toxic for plants (Reich, 1987; Matyssek et al., 2008). As the fluxes of ozone and water vapour are proportional to each other inside the stomata, ozone uptake can be estimated from the stomatal conductance to water vapour (gs, mmol m^{-2} s^{-1}) by multiplication with 0.668 (Laisk et al., 1989; UNECE, 2010). This enables to use e.g.

the multiplicative stomatal model by Jarvis (1976) to infer ozone uptake. Based on this multiplicative approach, Emberson et al. (2000) proposed the DO_3SE model (Deposition of Ozone for Stomatal Exchange) for estimation of ozone uptake from temperature, vapour pressure deficit (VPD), light and soil moisture. Future ozone control scenarios will rely on this approach (UNECE, 2004; Büker et al., 2007; Tuovinen et al., 2009). The DO_3SE model was tested by reanalyzing O_3 fumigation experiments and comparing the results to the AOT40 metric (Karlsson et al., 2004, Karlsson et al., 2007; Bueker et al., in prep.). This comparison showed that a flux based ozone metric may indeed improve the risk assessment. In analogy to the 40 ppb threshold in AOT40, a threshold of 1 nmol m^{-2} s^{-1}, below which detoxification processes are thought to be sufficient, was suggested for the DO_3SE model (UNECE, 2010). The ozone uptake model proved to be superior to the AOT40 approach in terms of visible symptoms in plants (Gerosa et al., 2008) and for biomass loss in experiments (Bueker et al., in prep.).

However, the parameters for the DO_3SE model have been compiled from a variety of sources, often laboratory experiments, and it is desirable to validate them with data from mature trees. It is also a matter of discussion if the model should include the change of stomatal conductance by ozone (UNECE, 2004; Pleijel et al., 2007). Ozone usually leads to stomatal closure in parallel to a reduction in photosynthesis (review by Wittig et al., 2007) but an impairment of the stomatal closure by ozone has also been observed (Maier-Maercker and Koch, 1991; Pearson and Mansfield, 1993; Paoletti, 2005).

The analogy between leaf transpiration and ozone uptake allows the use of sap flow measurements to validate ozone uptake models because they give a valid proxy of canopy conductance and can be run over a large range of meteorological conditions. As boundary layer resistance is rarely substantial in forests (Köstner et al., 1992), they give also a proxy for stomatal conductance. They integrate over the whole crown, but it is not always possible to get quantitative estimates of total water loss and absolute conductance values as this requires information on the distribution of water flux within the sapwood and on total leaf area (Cermák et al., 2004). However, even relative sap flow data can give useful information on stomatal behaviour. Sap flow data were used by Granier et al. (2000) to derive relationships between meteorological parameters and canopy conductance. The concept was further developed by Wieser et al. (2003, 2006, 2008), Nunn et al. (2007) and Köstner et al. (2008) to quantify the uptake of ozone and other trace gases. They multiplied the conductance to ozone calculated from sap flow measurements with the gas concentration in the air to get ozone uptake. The aim of the present investigation was to generalize this concept by deriving stomatal functions from sap flow measurements and to clarify whether the inclusion of O_3 as an additional modifier would be justified.

Materials and Methods

Sites

The measurements were perfomed in 3 beech stands (Table 1). The site in Hofstetten is described in more detail by Leuzinger et al. (2005). The external ozone concentration at Sagno (AOT40) is about 3-4 times higher than at Muri.

Meteorological measurements

In Muri and in Sagno, meteorological stations were run outside the forest, at a distance of 750m and 500 m, respectively. Temperature and humidity was measured using a Rotronic combined probe (Rotronic, Switzerland) in a ventilated housing which was calibrated once a year against NIST traceable standards. For global radiation, a LICOR pyranometer (LI-200SA-50; LICOR Nebraska USA) was used. To convert to photosynthetic active radiation, a factor of 2.057 was used which is derived from the factors given by Jones (1992) and Larcher (2003). Wind speed data were collected using a Young anemometer (model 05103) 2m above soil. Ozone was measured with TEI 49C monitors (Thermo Electron Corporation, USA) calibrated once a year using a transfer standard. Soil water potential was recorded using equitensiometers (Ecomatik, Dachau, Germany) in two different soil depths, the volumetric water content with theta probes (Delta-T) in one depth.

For the Hofstetten site, details can be found in Leuzinger et al.(2005). Meteorological data were monitored on top of a crane within the forest, above the canopy. Ozone data were available from a station 7.25 km north of the site (Schönenbuch) equipped with a TEI49C monitor. This station is situated in a comparable air pollution situation but because of the quite large distance its data were used for informative purposes only (estimate of total ozone uptake), not for regression analysis including ozone. Volumetric soil water content was measured during short periods. The data were used to calibrate the application of a soil water model (Schulla and Jasper, 2007) to the site. In order to avoid soil moisture limitation, data analysis in Hofstetten was restricted to days with a relative soil water saturation of 80%, assuming that this corresponds to a soil water potential where water starts to become limiting. As no data on soil water potential were available, Hofstetten was omitted from the analysis of the relation between sap flow and soil water.

Ozone concentrations from the monitoring stations were extrapolated to stand level as described in UNECE (2004).

Sap flow measurements

Sap flow of beech was measured using thermo dissipation probes (Granier, 1985) in Muri and Sagno between August 2003 and October 2005 during the season (Markasub, Olten, Switzerland). In Hofstetten, measurements lasted from April to September in 2004 and from June to September in 2005. The temporal resolution of the measurements was 30 minutes in Muri and Sagno and 10 minutes in Hofstetten, with the latter converted to 30 minute averages for reasons of comparability. The probes had a length of 55 mm, with the temperature measurement being performed at a depth of 27 mm. Because not enough information on the distribution of sap flux density within the sapwood and on leaf area per tree was available, the conductance data were converted to relative units for the data analysis by dividing through a 90th percentile for each season and tree. The 90th percentile was chosen to make the standardization more robust towards outliers.

Estimation of conductance

Sap flow measurements usually lag behind the driving meteorological condition by minutes or even hours because of the spatial separation of the probes from the stomata and because of water storage in the stem (Köstner et al., 1996; Zweifel and Häsler, 2001). For conductance estimations from sap flow, this time lag has to be considered. Examination of the data revealed that this lag was not constant; it tended to be higher on days with low flux speed. It was therefore determined for each tree separately using a daily regression between sap flow and lagged evapotranspiration which was calculated from temperature, radiation, VPD and wind speed using the Penman-Monteith equation. Only morning hours (6.00 to 13.00 hours) were used for this analysis as the reopening of stomata in the afternoon depends on the history of transpiration and often is much more difficult to explain (Körner, 1994). Optimum lag was assumed when R^2 reached its maximum. Because low R^2 or high lags are an indication of situations where meteorology does not explain sap flow conductance well enough, days with a R^2 of <0.95 or with a time lag of >1.5 hours were excluded from further analysis.

Total conductance was then estimated using the lagged sap flow according to Köstner et al.(1992):

$$g_t = (\rho * G_v * T_k) * E / VPD$$

with g_t: canopy conductance (mm s^{-1})

ρ: density of water (998 kg m^{-3})

G_v: gas constant for water vapour (0.462 m^3 kPa kg^{-1} K^{-1})

T_k: air temperature in K

E: sap flow density (mm h^{-1})

VPD: vapour pressure deficit (kPa)

Periods with a vapour pressure deficit (VPD) of < 0.5 hPa, where conductance estimation is subjected to large errors, or within 3 hours after rain were excluded from further analysis.

Statistics

All statistical analyses were performed using the software packages SYSTAT (SYSTAT Richmond, USA, version 11) and S-PLUS (TIBCO Software, Palo Alto, USA, version 8.1).

Fit to the envelope curve (model 1)

To get an estimation of the local optimum under a certain environmental condition (light, temperature or VPD), possibly without the constraints of the other variables, the independent variables were divided into 13-26 classes. Within each class, the 90^{th} percentile of conductance was determined per tree to obtain an estimate of the local maximum while excluding outliers from the analysis. This yielded an envelope curve of the conductances which was then normalized to a maximum of 1 within each tree to enable direct comparison (i.e., by dividing the 90^{th} percentile of each class by the maximum 90^{th} percentile in the respective tree). In the case of VPD, the data were normalized to the 90^{th} percentile value at 1 kPa instead of the maximum. For the analysis of slowly changing parameters such as soil water potential (SWP) and phenological stages, daily maxima for the hours 7-10 were used to estimate an envelope curve as above. Using nonlinear regression, a function was fitted through these normalized 90^{th} percentile values for each of the influencing variables temperature, light and VPD separately. The model was run with the Gauss-Newton procedure (SYSTAT module nonlin) in combination with the Hampel robust procedure.

Multivariate nonlinear regression (model 2)

For the multivariate nonlinear regression, the whole dataset with all single half hour values was subjected to data analysis, with the exceptions given below. An overall normalization was applied to the raw conductance values within each tree by dividing them by the 90th percentile of conductance within the respective tree before being processed further. Values which exceeded this 90th percentile by more than a factor of 2 were excluded from further analysis. This procedure enabled direct comparison of trees of different size and prevented outliers from affecting the data analysis.

The half hour conductance data which had been transformed as outlined above were then subjected to a two stage nonlinear regression with simultaneous estimation of the functions for light, temperature and VPD in S-PLUS, treating the individual trees as groups (Pinheiro and Bates, 2000). In the first stage, a non-linear model was fitted for each tree using the function nlsList. In the second stage, weighted means of the tree-specific parameter estimates were computed, with each weight being inversely proportional to the sum of the square of the respective standard error and the variance of the random effect describing the degree of heterogeneity between trees. This allowed the consideration of the grouped data structure and enabled convergence of the nonlinear regression with the full dataset. The function for soil water was kept constant.

The structure of the equation fitted was:

$$f_s = f_{phen} \times f_{light} \times \{(f_{temp} \times f_{VPD} \times f_{SWP} \times f_{O_3}) + f_{\min}\} + error \qquad (1)$$

The functions for f_{phen}, f_{light}, f_{temp}, f_{VPD} and f_{O3} are non-linear in their respective predictor variable and will be described in the result section.

Our analysis did not account for serial correlation of outcome data within trees. This probably led to an underestimation of the standard errors of parameter estimates. On the other hand, the large heterogeneity between trees was the dominating influence in the meta-analysis anyway, tending to shrink meta-analytic estimates toward arithmetic means.

DO3SE model

The uptake model for beech (UNECE, 2004) was used to calculate ozone uptake to enable a comparison with the model results presented in this paper. The 2009 parameterization for beech was used (Table 2).

Estimation of ozone uptake

Both the envelope and the multivariate models yielded scaling factors for light, temperature, VPD and SWP which were then combined to a single factor between 0 and 1 according to equation 1. The resulting relative conductance was compared with the relative conductance values obtained by scaling the sap flow data which also extend between 0 and 1. These relative values were multiplied with a maximum conductance to ozone, g_{max}, of 150 mmol m^{-2} s^{-1}. Ozone uptake was then estimated for each tree and each time step by multiplying the values of stomatal conductance provided by the respective model with the concurrent ambient ozone concentration. An hourly flux threshold of 1 nmol m^{-2} s^{-1} was subtracted in the case of the threshold cumulative uptake (UNECE, 2010). The functions for soil water and the growing season were kept similar for all models to facilitate direct comparison. The estimates of ozone uptake from the two models, along with the DO_3SE estimates, were contrasted with the ones obtained directly from sap flow measurements. These calculations were done for the whole day (i.e. including the afternoon hours).

Phenological stages

The Swiss phenology dataset (Defila, 1986) was used for the determination of budbreak and leaf fall. They were used in the definition of the growing season and in the derivation of a function for phenology.

Results

Time lag

Time lag was not constant. It varied between 0 and ≥4 hours (≥ 8 half hourly means) (Figure 1). Days with time lags of more than 1.5 hours or with an insufficient regression between sap flow and evaporation (R^2 of <0.95) were excluded from the analysis. This reduced the dataset by 31%. This determination of time lag was purely empirical. It was not possible to find a model explaining a sufficient proportion of its variation.

Model 1: Fit of the envelope curve

Temperature

The following function was used to fit the data (Emberson et al., 2000):

$$f_{temp} = \left(\frac{T - T\min}{Topt - T\min} \right) \times \left(\frac{T\max - T}{T\max - Topt} \right)^{bt} \quad (2)$$

The results of fitting equation 1 to the data points are listed in Table 4. Optimum temperature (T_{opt}) was estimated to be 15.0°C, minimum (T_{min}) at 5.0° and the maximum (T_{max}) to 41.2° .

Vapour pressure deficit

According to Oren et al.(1999), an equation was fitted which is based on the conductance at a VPD of 1 kPa (gs_{ref}). However, a negative exponential function instead of the original log function was chosen to avoid values below zero. Here, gs_{ref} is set to 1 and the relative conductance values were scaled to 1 at 1 kPa (Figure 3). The resulting parameter is listed in Table 4.

$$f_{VPD} = e^{m*(1-VPD)} \qquad (3)$$

Radiation

The function proposed by Emberson et al.(2000) was fitted:

$$g_{light} = 1 - e^{(PAR \times light_a)} \qquad (4)$$

For the estimation, only PFD values <1000 μmol were considered. At higher values the conductance is decreasing again because of high VPD values co-occurring with high light intensities (Figure 4). The resulting parameter is listed in Table 4.

Soil moisture deficit

The conductance decreased with decreasing water availability of the soil which was measured at a depth of 40 cm. The relation seems more or less linear (Figure 5). The fitted line has a slope of 0.91 (confidence interval 0.22 to 1.59). The regression with data from 20 cm depth was not significant (data not shown).

Model 2: Multivariate nonlinear estimate

Because of the intercorrelations between the predictor variables and in order to test if ozone concentrations affected stomatal conductance, another procedure was tested with simultaneous estimation of all parameters except for soil water (f_{SWP}) for which the relation shown in Figure 5 was used. The temperature equation had to be modified to achieve convergence of the nonlinear multiple regression model. In this new equation, b_1 and the optimum temperature (T_{opt}) are the regression coefficients to be estimated, T is air temperature in °C:

$$f_{temp} = e^{b_1 * (T - T_{opt})^2} \qquad (5)$$

The functions for light and for VPD were not changed. An overall scaling factor (c) was introduced to compensate for differences in the scaling of the individual trees. This was needed to achieve convergence of the nonlinear model.

For mathematical and interpretational reasons, O_3 was centered to the average (50 ppb), i.e. 50 was subtracted from all ozone concentrations. This reduces the confidence interval of the intercept.

The term for ozone had the following form:

$$f_{O_3} = e^{\delta * O_3} \qquad (6)$$

with δ being the coefficient for the ozone function to be estimated.

The overall equation fitted was:

$$f_s = c \times \left[1 - e^{(PAR \times light_a)}\right] \times \left\langle \left[e^{m \times (1 - VPD)}\right] \times \left[e^{(b_1 \times (T - T_{opt})^2)}\right] \times e^{\delta \times O_3} \times f_{SWP} + f_{\min} \right\rangle \qquad (7)$$

The coefficient for O_3 was not significant (p=0.74). Its inclusion changed, however, the fits for temperature, suggesting a serious problem with collinearity. The analysis was therefore repeated replacing the ozone data with residuals of a regression of ozone against temperature and radiation. The result was also nonsignificant (P=0.86). When the maximum ozone concentration of the previous day was used as a measure for ozone, there was a trend for a negative correlation (6 out of 8 trees with negative coefficients) but overall conversion was not achieved. As the ozone term was difficult to quantify and because of the problems with confounding meteorology, it was removed from the equation.

The parameter estimates of the remaining multiple non-linear regression model are listed in Table 5.

Model comparisons

The regression curves corresponding to the parameters in Table 5 are shown in Figure 2, Figure 3, and Figure 4 (grey line), in comparison to the functions resulting from model 1 (black line). The multivariate data analysis causes the optimum temperature to shift from 15.0° to 23.2°C. On the other hand, the VPD function decreases more rapidly, with conductance values of <0.1 reached already at 2.65 kPa instead of 5.24.

The VPD function presented here does not fulfil the criteria of the DO_3SE model to accept values between 0 and 1. This causes, however, rarely a problem as low VPD values usually co-occur with low light levels which limit conductance. In fact, the resulting average conductance showed an optimum around 1 kPa (Figure 5). The figure highlights also that the envelope curve model does not include a term for f_{min}.

Estimation of ozone flux

Ozone uptake was estimated by multiplying ozone concentrations, a g_{max} of 150 nmol m^{-2} s^{-1} (UNECE, 2010) and relative conductance values. The latter were calculated either directly from sap flow as reference or from the different models (for model 1: Table 4, for model 2: Table 5). Total cumulative ozone uptake was summed up for each tree and each year separately for periods with valid sap flow data, both without (Figure 7) and with a threshold of 1 nmol m^{-2} s^{-1} (Figure 8). The envelope model seriously underestimates the ozone uptake both with and without a threshold (on average by 34 and 37%, respectively) (Table 6). On average, the predictions for flux without threshold from the multivariate model fit very well; with a threshold of 1 they are too high by 26%. The estimate by the DO_3SE model was included for comparison. DO3SE has a somewhat higher scatter (lower R^2) and overestimates the flux, moderatly without (10%) and substantially with threshold (39%). The results also suggest that it is more difficult to get a good estimate when a threshold is considered in the ozone uptake calculation.

The difference between ozone uptake from sapflow and modelled uptake was plotted against several predictors to test for systematic deviations (Figure 9). For this test, the differences of the daily cumulative uptake of ozone were used, the 24h-average of temperature (b) and the maximum half hourly mean of VPD (c) and ozone (d), respectively. It was also plotted against the measured soil water potential (f). Whereas the envelope model seriously underestimates the flux at medium temperatures, medium VPD’s and high ozone values, there are less systematic deviations in the case of the multivariate model. The DO_3SE model performs almost as well as the multivariate model.

Bud break and seasonal variation

The sap flow measurements were conducted during the whole season. Therefore it was possible to follow a seasonal variation. The increase of conductance after budbreak can be described by a Michaelis-Menten function, with a K-value of 8.7 (95% confidence interval 3.11-14.29) (Figure 10). This means that 50% of the conductance is reached 9 days after budbreak. Between 50 and 150 days after budbreak there is not much variation of conductance (data not shown).

$$gphen = \frac{v\max * D}{k + D} \qquad (8)$$

with:

vmax: maximum conductance (set to 1.18 to reach a value of 1 after 50 days)

D: number of days since budbreak.

k: Michaelis-Menten constant

After 50 days, a constant value of 1 was used till the end of the season.

Recommendations for calculation of ozone uptake

For calculation of ozone uptake, it is recommended to take the results from the multivariate (model 2). The following overall function is suggested:

$$f_s = f_{phen} \times f_{light} \times \{(f_{temp} \times f_{VPD} \times f_{SWP}) + f_{\min}\} \qquad (9)$$

$$f_{light} = 1 - e^{(PAR \times light_a)} \qquad (10)$$

with $light_a$=-0.00112 and PAR in µmol m^{-2} s^{-1}

$$f_{temp} = e^{b_1 * (T - T_{opt})^2} \qquad (11)$$

with b_1=-0.00502 and T_{opt}=26.49

$$f_{VPD} = e^{m \times (1 - VPD)} \qquad (12)$$

with m=1.39 and VPD in kPa

$$f_{SWP} = 1 - a * SWP \qquad (13)$$

with a=1.1 and SWP in MPa.

F_{min} was estimated to be 0.20. It has, however, to be born in mind that the Granier sap flow measurements do not allow to determine a true minimum.

For the start of the growing season, the following equation is suggested, with D being the difference between Julian date and SGS:

$$f_{phen} = \begin{cases} 0 & when\ day < SGS\ or\ day > EGS \\ \dfrac{1.18 * D}{k + D} & when\ day \geq SGS\ and < (SGS + 50) \\ 1 & when\ day > (SGS + 50) \end{cases} \qquad \text{with k=8.70}$$

Discussion

The data suggest that the analysis of sap flow data is a useful tool to derive response functions of stomata to environmental variables. In contrast to direct conductance measurements in the crown (usually sun leaves), sap flow integrates over the whole crown including the shade leaves and includes also boundary layer resistance (Köstner et al., 1992). A large dataset, which is usually provided by continuous measurements, allows also the evaluation over a large range of meteorological conditions. The multivariate model gave the better estimates as it accounts for collinearity between the predictors.

Temperature

The difference in the temperature optimum between the envelope and the multivariate model is probably the result of co-occurring high VPD values at higher temperature and reflects the difficulties to determine a real optimum under field conditions. With porometer measurements, Gerosa et al. (2008) observed a higher temperature optimum of stomatal conductance of young *Fagus sylvatica* in Northern Italy (27°C), but also a high minimum temperature (12°C) which is beyond the range presented in this study. He explains this higher temperature optimum with the southern Alpine origin of the ecotype. The results of model 1 are in good agreement with the results from Nunn et al. (2005) obtained by porometer measurements. For sun leaves of mature beech, they found a T_{min} of 8°C, T_{opt} of 21°C and T_{max} of 34°C, whereas for shade leaves the corresponding parameters were 0°C, 15°C and 30°C. Using sap flow measurements, Granier et al. (2000a) observed a strong limitation of the canopy conductance at air temperatures below 15-17°C and assumed a T_{min} value of 10°C for the Euroflux beech sites Hesse and Aubure. Their conductance values stayed high till 30°C, so T_{max} was certainly higher than the value found in this study. Osonubi and Davies (1980) observed the highest stomatal conductance of birch seedlings at 20°C when they used a constant VPD setting during their measurements. Photosynthesis had a higher temperature optimum. They explain the difference in temperature optimum between the conductance and photosynthesis by a lower temperature optimum for metabolism in the guard cells than for photosynthesis in the mesophyll cells.

VPD

The current DO_3SE model for beech uses a stepwise linear VPD function with values of 1 between 0 and 0.93 kPa (=VPD_{max}), in some tree species even up to higher VPD values. Emberson et al. (2000) or Nunn et al. (2005) suggest a VPD_{max} of 1.1 kPa, Gerosa et al. (2008) even of 1.8 kPa (for *Fagus sylvatica*). Körner (1994) summarizes several studies for various tree species with VPD thresholds of 0.5-1.2 kPa, mostly around 1. Kerstiens (1995) observed a linear behaviour of stomatal resistance in beech saplings between 0.6 and 3 kPa, without an indication of a threshold value within this range. Continuous monitoring of canopy conductance including VPD below these thresholds yields, however, rather a negative exponential function with values strongly decreasing between 0 and 1 kPa: Granier et al. (2000b) with sap flow, Kutsch et al. (2001) with a stationary gas exchange system and Herbst (1995) with Bowen ratio measurements. As porometer measurements are usually made on clear, sunny days and therefore rarely at low VPD values, this also poses the question how to define g_{max}. Oren et al.(1999) therefore proposed to normalize the conductance to a VPD value of 1 kPa (gs_{ref}) and fitting a log function which allows to assume values greater than 1 at VPD < 1kPa. In this study, this was modified to a negative exponential function which yielded better conversion results than other functions tested and does not take values <0. Inspite of the steady decrease of the VPD function, the resulting modelled conductance values show a maximum at a VPD of about 0.5 kPa which is probably a result of low light intensities co-occurring with low VPD. The observed response of conductance to VPD may depend on the method used for sap flow measurement or the insertion depth of the sensors. Köstner et al. (1996), comparing three different sap flow systems, found that the Granier system used in this study yielded the strongest relationship between conductance and VPD. The VPD threshold also seems to vary with environmental variables. Heath (1998) observed that the stomata of 2-year-old seedlings of beech and chestnut growing in elevated CO_2 (+250 ppm) failed to close normally in response to increased VPD. Kutsch et al. (2001) suggests seasonal differences of the VPD response. It is, however, not clear if these differences are caused by a decreased overall conductance which changes the level of comparison or if it is a real change of response.

Light function

The light curve of the multivariate model does not reach saturation at ambient light levels which is a violation of the model concept. The resulting ozone uptake showed, however, no systematic deviations at various light levels and seems to be more realistic than the one estimated with the envelope model although the light function from the latter is in excellent agreement with studies using single leaves or laboratory measurements. Gerosa et al. (2008) derived a coefficient of -0.007 from porometer measurements in young *Fagus sylvatica*. From the data published by Kutsch et al. (2001) for a low VPD a coefficient of -0.0067 can be derived. Nunn et al. (2005) used a coefficient of -0.006 for sun leaves and of -0.06 for shade leaves. When comparing coefficients from laboratory to field studies, it has to be born in mind that field measurements such as sap flow integrate over the whole crown, with various shading patterns for different parts of the crown. A slower increase was observed by Herbst (1995) when analysing the transpiration of a whole beech stand using Bowen ratio. Bulk stomatal conductance did not reach light saturation until 1200 μmol m^{-2} s^{-1} at low VPD or even higher values at high VPD. This is in accordance with the results of the current study.

Minimum conductance (f_{min})

Sap flow measurements with the Granier method do not allow to determine a true minimum as the nighttime temperature differences are used to set zero flux. Nighttime transpiration may, however, be substantial. A compilation of data from different ecosystems suggests values between 3 and 17% of daytime conductance (Dawson et al., 2008). Modifications of the analysis of Granier data to allow for a more exact determination of nighttime transpiration have been proposed by Regalado and Ritter (2007) but it was not possible to apply this method in the current dataset. Thus, the relative conductance has to be increased by a constant value. The f_{min} term obtained in the multivariate analysis is an estimate for a daytime minimum, not for nighttime transpiration.

Ozone

Maximum ozone concentrations of the preceding day seemed to decrease stomatal conductance, whereas no relation was observed with the current ozone concentration. The strong collinearity of ozone with temperature, irradiation and VPD makes it, however, very difficult to get reliable evidence of an ozone effect on conductance. This highlights also the limits of a multivariate approach with field data. Wittig et al. (2007) compiled 30 years of fumigation experiments and found a general decrease of stomatal conductance by ozone fumigation, with the exception of conditions of drought which is explained by a protective effect of drought against ozone uptake. However, a stomatal closure in response to ozone is not always observed. By comparing *Pinus jeffreyi* on microsites with different water regimes, Grulke et al. (2003) were not able to clearly corroborate a protective effect of drought from O_3 uptake. McLaughlin et al. (2007) reported increased sap flow velocity in red oak (*Quercus rubra*), hickory (*Carya sp.*), yellow poplar (*Liriodendron tulipifera*) and pitch pine (*Pinus rigida*) when O_3 concentrations were high. This was paralleled by an increased loss of soil moisture. It is, however, not clear how the effects of ozone and of confounding ozone promoting meteorological conditions were separated in this study. Grulke et al. (2008) also observed an increased stomatal conductance at higher ozone concentrations in *Fagus sylvatica*. Impaired stomatal control as a consequence of ozone has been reported by Pearson and Mansfield (1993) for beech, by Maier-Maercker and Koch (1991) for Norway spruce and by Paoletti (2005) for a Mediterranean evergreen broadleaf species.

Soil water

It is difficult to make representative soil water potential measurements within the root zone. Therefore it is not surprising that the relationship between conductance and soil water potential was not very strong. However, the observed relationship agrees with assumptions based on soil physics. The extrapolation of the line intersects a low limit of conductance of 0.1 at a value of -0.99 Mpa. Although this value is higher than the permanent wilting point of -1.5 MPa, which is assumed to be the lower end of water availability for plants, it is still in agreement with this theoretical background as the error of the estimate is quite large. Nunn et al. (2005) used -0.05 for SWP_{min} and -1.25 Mpa for SWP_{max} . The response to soil water deficit may be subjected to genetical modification: Tognetti et al. (1995) found different responses in beech seedlings with provenance from Northern Italy or Sicily. For large scale modelling purposes, SWP is not a convenient parameter as the relationship between the calculated volumetric soil water content and the water potential is nonlinear and depends not only on texture but also on other soil properties. A comparison between measured SWP and modelled soil moisture deficit suggested that the latter is also a useful parameter to predict stomatal conductance (data not shown). But it has also to be stated here that soil moisture deficit is also highly correlated with low VPD.

Conclusions

Our sap flow analysis supports earlier results gained in beech with other methods. The multivariate nonlinear regression analysis allows to deal with serious collinearity as generally observed in meteorological data and is a powerful tool to extend the uptake calculations for other tree species. The data also corroborate the current parameterization of the DO_3SE model for beech.

Acknowledgements

The present work was supported by the Federal Office for Environment. We thank Beat Achermann for the support and his interest in the work, Giuseppe Tettamanti and Beat Bossert for allowing us to measure in their nurseries and in the forest. The technical assistance of Roland Woëffray, Dieter Bader and Michael Tobler is acknowledged as well. We thank also Christian Körner and Raphael Mainiero for helpful discussions on the manuscript, the Swiss Meteorological Institute (Claudio Defila, Thomas Herren) for the supply with phenological data and the staff from TIBCO (SPLUS support) for support in the application of nonlinear regression.

References

Braun, S., Flückiger, W., 1989. Effect of ambient ozone and acid mist on aphid development. Environmental Pollution 56, 177-187.

Braun, S., Schindler, C., Rihm, B., Flückiger, W., 2007. Shoot growth of mature *Fagus sylvatica* and *Picea abies* in relation to ozone. Environmental Pollution 146, 624-628.

Büker, P., Emberson, L. D., Ashmore, M. R., Cambridge, H. M., Jacobs, C. M. J., Massman, W. J., Müller, J., Nikolov, N., Novak, K., Oksanen, E., Schaub, M., de la Torre, D., 2007. Comparison of different stomatal conductance algorithms for ozone flux modelling. Environmental Pollution 146, 726-735.

Cermák, J., Kucera, L. J., Nadezhdina, N., 2004. Sap flow measurements with some thermodynamic methods, flow integration within trees and scaling up from sample trees to entire forest stands. Trees 18, 529-546.

Dawson, T. E., Burgess, S. S. O., Tu, K. P., Oliveira, R. S., Santiago, L. S., Fisher, J. B., Simonin, K. A., Ambrose, A. R., 2008. Nighttime transpiration in woody plants from contrasting ecosystems. Tree Physiology 27, 561-575.

Defila, C., 1986. Phänologische Beobachtungen in der Schweiz (gestern - heute - morgen). Arboreta Phaenologica 31, 61-69.

Emberson, L. D., Ashmore, M. R., Cambridge, H. M., Simpson, D., Tuovinen, J.-P., 2000. Modelling stomatal ozone flux across Europe. Environmental Pollution 109, 403-414.

Fowler, D., Cape, J. N., Coyle, M., Flechard, C., Kuylenstierna, J., Hicks, K., Derwent, D., Johnson, C., Stevenson, D., 1999. The global exposure of forests to air pollutants. Water Air and Soil Pollution 116, 5-32.

Fuhrer, J., Achermann, B., 1999. Critical levels for ozone - level II. Workshop under the Convention on Long-Range Transboundary Air Pollution of the United

Nations Economic Commission for Europe (UN/ECE), Gerzensee, Switzerland, 11-15 April 1999. Environmental documentation 115 333pp, Swiss Agency for the Environment, Forests and Landscape (SAEFL), Berne.

Fuhrer, J., Skärby, L., Ashmore, M. R., 1997. Critical levels for ozone effects on vegetation in Europe. Environmental Pollution 97**,** 91-106.

Gerosa, G., Marzuoli, R., Desotgiu, R., Bussotti, F., Ballarin-Denti, A., 2008. Visible leaf injury in young trees of Fagus sylvatica L. and Quercus robur L. in relation to ozone uptake and ozone exposure. An Open-Top Chambers experiment in South Alpine environmental conditions. Environmental Pollution 152**,** 274-284.

Granier, A., 1985. Une nouvelle méthode pour la mesure du flux de sève brute dans la tronc des arbres. Annales des Sciences forestières 42**,** 193-200.

Granier, A., Biron, P., Lemoine, D., 2000a. Water balance, transpiration and canopy conductance in two beech stands. Agricultural and Forest Meteorology 100**,** 291-308.

Granier, A., Loustau, D., Bréda, N., 2000b. A generic model of forest canopy conductance dependent on climate, soil water availability and leaf area index. Annales des Sciences forestières 57**,** 755-765.

Grulke, N. E., Grams, T. E. E., Paoletti, E., Nunn, A. J., Häberle, K. H., Matyssek, R., 2008. Kinetics of stomatal and assimilation response to short term changes in O_3 concentration in mature *Fagus sylvatica* trees grown at ambient or long-term elevated O_3 . 23rd IUFRO meeting for Specialists in Air Pollution Effects on Forest Ecosystems, 7.-12. September 2008, Murten, Switzerland.

Grulke, N. E., Johnson, R., Esperanza, A., Jones, D., Nguyen, T., Posch, S., Tausz, M., 2003. Canopy transpiration of Jeffrey pine in mesic and xeric microsites: O3 uptake and injury response. Trees 17**,** 292-298.

Günthardt-Goerg, M., Matyssek, R., Scheidegger, C., Keller, T., 1991. Bioindikation in Birkenblättern unter niedrigen Ozonkonzentrationen. VDI.-Berichte. 901, 631-645.

Heath, J., 1998. Stomata of trees growing in CO2-enriched air show reduced sensitivity to vapour pressure deficit and drought. Plant, Cell and Environment 21, 1077-1088.

Herbst, M., 1995. Stomatal behaviour in a beech canopy: an analysis of Bowen ratio measurements compared with porometer data. Plant, Cell and Environment 18, 1010-1018.

Jarvis, P. G., 1976. The interpretation of the variations in leaf water potential and stomatal conductance found in canopies in the field. Philosophical Transactions of the Royal Society, London 273, 593-610.

Jones, H. G., 1992. Plants and microclimate. A quantitative approach to environmental plant physiology, Cambridge University Press, Cambridge.

Kärenlampi, L., Skärby, L., 1996. Critical Levels for Ozone in Europe. Testing and Finalizing the Concepts, University of Kuopio, Dep. of Ecology and Environmental Science.

Karlsson, P. E., Braun, S., Broadmeadow, M., Elvira, S., Emberson, L. D., Gimeno, B., LeThiec, D., Novak, K., Oksanen, E., Schaub, M., Uddling, J., Wilkinson, M., 2007. Risk assessment for forest trees: the performance of the ozone flux versus the AOT concepts. Environmental Pollution 146, 608-616.

Karlsson, P. E., Uddling, J., Braun, S., Broadmeadow, M., Elvira, S., Gimeno, B., Le Thiec, D., Oksanen, E. J., Vandermeiren, K., Wilkinson, M., Emberson, L. D., 2004. Dose - response relationships for ozone impact on the biomass accumulation of young trees of different European species based on AOT40 and cumulative leaf uptake of ozone. Atmospheric Environment 38, 2283-2294.

Kerstiens, G., 1995. Cuticular water permeance of European trees and shrubs grown in polluted and unpolluted atmospheres, and its relation to stomatal response to humidity in beech (*Fagus sylvatica* L.). New Phytologist 129, 495-503.

Körner, C., 1994. Leaf diffusive conductances in the major vegetation types of the globe, in: Schulze, E. D., Caldwell, M. M. (Eds.), Ecophysiology of Photosynthesis. Springer, pp. 463-490.

Köstner, B., Biron, P., Siegwolf, R., Granier, A., 1996. Estimates of water vapor flux and canopy conductance of Scots pine at the tree level utilizing different xylem sap flow methods. Theoretical and Applied Climatology 53, 105-113.

Köstner, B., Matyssek, R., Heilmeier, H., Clausnitzer, F., Nunn, A. J., Wieser, G., 2008. Sap flow measurements as a basis for assessing trace-gas exchange of trees. Flora 203, 14-33.

Köstner, B. M. M., Schulze, E. D., Kelliher, F. M., Hollinger, D. Y., Byers, J. N., Hunt, J. E., McSeveny, T. M., Meserth, R., Weir, P. L., 1992. Transpiration and canopy conductance in a pristine broad-leaved forest of Nothofagus: an analysis of xylem sap flow and eddy correlation measurements. Oecologia 91, 350-359.

Kutsch, W., Herbst, M., Vanselow, R., Hummelshøi, P., Jensen, N. O., Kappen, L., 2001. Stomatal acclimation influcences water and carbon fluxes of a beech canopy in northern Germany. Basic and Applied Ecology 2, 265-281.

Laisk, A., Kull, O., Moldau, H., 1989. Ozone concentraton in leaf intercellular air spaces is close to zer. Plant Physiology 90, 1163-1167.

Landeshydrologie, 1992. Hydrologischer Atlas der Schweiz, Bundesamt für Wasser und Geologie, Bern.

Larcher, W., 2003. Physiological Plant Ecology: Ecophysiology and Stress Physiology of Functional Groups, Springer, Berlin.

Leuzinger, S., Zotz, G., Asshoff, R., Körner, C., 2005. Responses of deciduous forest trees to severe drought in Central Europe. Tree Physiology 25, 641-650.

Maier-Maercker, U., Koch, W., 1991. Experiments on the control capacity of stomata of *Picea abies* (L.) Karst. after fumigation with ozone and in environmentally damaged material. Plant, Cell and Environment 14, 175-184.

Matyssek, R., Sandermann, H., Wieser, G., Booker, F., Cieslik, S., Musselman, R., Ernst, D., 2008. The challenge of making ozone risk assessment for forest trees more mechanistic. Environmental Pollution 156, 567-582.

McLaughlin, S. B., Kohut, R. J., 1992. The effects of chemosphere deposition and ozone on carbon allocation and associated physiological processes, in: Eagar, C., Adams, M. B. (Eds.), Ecology and decline of red spruce in the eastern United States. Springer Verlag, pp. 338-382.

McLaughlin, S. B., Wullschleger, S., Sun, G., Nosal, M., 2007. Interactive effects of ozone and climate on water use, soil moisture content and streamflow in a southern Appalachian forest in the USA. New Phytologist 174, 125-136.

Nunn, A. J., Kozovits, A. R., Reiter, I. M., Heerdt, C., Leuchner, M., Lütz, C., Liu, X., Löw, M., Winkler, J. B., Grams, T. E. E., Häberle, K. H., Werner, H., Fabian, P., Rennenberg, H., Matyssek, R., 2005. Comparison of ozone uptake and sensitivity between a phytotron study with young beech and a field experiment with adult beech (*Fagus sylvatica*). Environmental Pollution 137, 494-506.

Nunn, A. J., Wieser, G., Metzger, U., Löw, M., Wipfler, P., Häberle, K. H., Matyssek, R., 2007. Exemplifying whole-plant ozone uptake in adult forest trees of contrasting species and site conditions. Environmental Pollution 146, 629-639.

Oren, R., Sperry, J. S., Katul, G. G., Pataki, D. E., Ewers, B. E., Phillips, N., Schäfer, K. V. R., 1999. Survey and synthesis of intra- and interspecific variation in stomatal sensitivity to vapour pressure deficit. Plant, Cell and Environment 22**,** 1515-1526.

Osonubi, O., Davies, W. J., 1980. The influence of water stress on the photosynthetic performance and stomatal behaviour of tree seedlings subjected to variation in temperature and irradiance. Oecologia 45**,** 3-10.

Paoletti, E., 2005. Ozone slows stomatal response to light and leaf wounding in a Mediterranean evergreen broadleaf, *Arbutus unedo*. Environmental Pollution 134**,** 439-445.

Pearson, M., Mansfield, T. A., 1993. Interacting effects of ozone and water stress on the stomatal resistance of beech (*Fagus sylvatica* L.). New Phytologist 123**,** 351-358.

Pinheiro, J. C., Bates, D. M., 2000. Mixed-Effects Models in S and S-PLUS. Statistics and Computing Springer-Verlag, New York.

Pleijel, H., Danielsson, H., Emberson, L. D., Ashmore, M. R., Mills, G., 2007. Ozone risk assessment for agricultural crops in Europe: Further development of stomatal flux and flux-response relationships for European wheat and potato. Atmospheric Environment 41**,** 3022-3040.

Regalado, C. M., Ritter, A., 2007. An alternative method to estimate zero flow temperature differences for Granier's thermal dissipation technique. Tree Physiology 27**,** 1093-1102.

Reich, P. B., 1987. Quantifying plant response to ozone: a unifying theory. Tree Physiology 3**,** 63-91.

Samuelson, L., Kelly, J. M., 1996. Carbon partitioning and allocation in northern red oak seedlings and mature trees in response to ozone. Tree Physiology 16, 853-858.

Schulla, J., Jasper, K., 2007. Model description Wasim-ETH, http://homepage.hispeed.ch/wasim/ November 2007, Zürich.

Sitch, S., Cox, P. M., Collins, W. J., Huntingford, C., 2007. Indirect radiative forcing of climate change through ozone effects on the land-carbon sink. Nature 448, 791-794.

Skärby, L., Ro-Poulsen, H., Wellburn, F. A. M., Sheppard, L. J., 1998. Impacts of ozone on forests: a European perspective. New Phytologist 139, 109-122.

Tognetti, R., Johnson, J. D., Michelozzi, M., 1995. The response of European beech (*Fagus sylvatica* L.) seedlings from two Italian populations to drought and recovery. Trees 9, 348-354.

Tuovinen, J. P., Emberson, L., Simpson, D., 2009. Modelling ozone fluxes to forests for risk assessment: status and prospects. Annals of Forest Science 66, Article.

UNECE, 2004. Manual on methodologies and criteria for modelling and mapping critical loads and levels and air pollution effects, risks and trends.

UNECE, 2010. Mapping Critical Levels for Vegetation, International Cooperative Programme on Effects of Air Pollution on Natural Vegetation and Crops, Bangor, UK.

Van Dingenen, R., Dentener, F. J., Raes, F., Krol, M. C., Emberson, L., Cofala, J., 2009. The global impact of ozone on agricultural crop yields under current and future air quality legislation. Atmospheric Environment 43, 604-618.

Wellburn, F. A. M., Wellburn, A. R., 1994. Atmospheric ozone affects carbohydrate allocation and winter hardiness of *Pinus halepensis* Mill. Journal of Experimental Botany 45**,** 607-614.

Wieser, G., Luis, V. C., Cuevas, E., 2006. Quantification of ozone uptake at the stand level in a *Pinus canariensis* forest in Tenerife, Canary Islands: An approach based on sap flow measurements. Environmental Pollution 140**,** 383-386.

Wieser, G., Matyssek, R., Köstner, B., Oberhuber, W., 2003. Quantifying ozone uptake at the canopy level of spruce, pine and larch trees at the alpine timberline: an approach based on sap flow measurements. Environmental Pollution 126**,** 5-8.

Wieser, G., Matyssek, R., Then, C., Cieslik, S., Paoletti, E., Ceulemans, R., 2008. Upscaling ozone flux in forests from leaf to landscape. Italian Journal of Agronomy 3**,** 35-41.

Wittig, V. E., Ainsworth, E. A., Long, S. P., 2007. To what extent do current and projected increases in surface ozone affect photosynthesis and stomatal conductance of trees? A meta-analytic review of the last 3 decades of experiments. Plant, Cell and Environment 30**,** 1150-1162.

Zweifel, R., Häsler, R., 2001. Dynamics of water storage in mature subalpine *Picea abies*: temporal and spatial patterns of change in stem radius. Tree Physiology 21**,** 561-569.

Tables

Table 1: Description of field sites. Rainfall values modelled from Landeshydrologie (1992).

										Ozone (AOT40 daylight, April-September)		
site	stand	Lat. (°)	Long. (°)	Rainfall (average 1981-2000) (mm)	Altitude (m)	Stand age (years)	Soil type	soil texture	stones	2003	2004	2005
Hofstetten	deciduous mixed	47.47	7.51	1200	540	95	leptosole	silty loam	accessible profile depth 30 cm	34.7*	15.5*	13.1*
Muri	pure beech	47.27	8.35	1138	490	125	cambisole	silty loam	30 vol% stones down to 70 cm, 70 vol% below	14.5	12.8	12.2
Sagno	pure beech	45.86	9.06	1660	770	80	leptosole	silty-clay loam	5 vol% stones down to 25 cm, 70 vol% below	48.6	36.9	48.2

* ozone values from Schönenbuch (7.25 km north).

Table 2: Parameterization of the DO3SE model used for comparison (UNECE, 2010)

f_{min}	0.13
g_{max}	150
$light_a$	-0.006
vpd_{min}	3.1
vpd_{max}	1.0
t_{max}	33
t_{opt}	16
t_{min}	5

Table 3: Abbreviations used

g_{max}	maximum conductance to ozone (mmol m^{-2} s^{-1})
PAR	photosynthetic active radiation μmol m^{-2} s^{-1})
VPD	vapour pressure deficit (kPa)
T	air temperature (°C)
O_3	ozone concentration (μl l^{-1}), centered to the overall average (50 subtracted)
SWP	soil water potential (MPa)
b_1	parameter for the temperature function
T_{opt}, T_{min}, T_{max}:	Optimum, minimum and maximum air temperature (°C)
m	parameter for the VPD function
$light_a$	parameter for the light function
δ	parameter for the O_3 function
POD0	phytotoxic ozone dose without threshold (mmol m^{-2}): ozone uptake accumulated for one season
POD1	phytotoxic ozone dose (mmol m^{-2}) with a threshold of 1 nmol m^{-2} s^{-1}
f_s	overall factor for conductance to ozone (between 0 and 1)
f_{phen}	factor for phenological stage
f_{light}	factor for light
f_{min}	factor for minimum conductance
f_{temp}	factor for temperature
f_{VPD}	factor for vapour pressure deficit (VPD)
f_{O3}	factor for ozone concentration
f_{SWP}	factor for soil water potential (SWP)

Table 4: Estimates from the envelope model

Function	R^2	Parameter	Estimate	95% confidence interval lower	upper
Temperature	0.765	T_{min}	5.0	4.2	5.9
		T_{opt}	15.0	12.7	17.4
		T_{max}	41.2	28.6	53.8
		bt	2.61	0.85	4.37
VPD	0.821	m	0.543	0.385	0.700
light	0.900	$light_a$	-0.00529	-0.00649	-0.00408

Table 5: Estimates from the simultaneous nonlinear estimate

Parameter	Estimate	95% confidence interval		p-value
$light_a$	-0.00112	-0.00157	-0.00067	<0.001
m	1.388	1.089	1.686	<0.001
b_1	-0.00502	-0.00641	-0.00363	<0.001
T_{opt}	26.49	23.12	29.87	<0.001
f_{min}	0.200	0.110	0.292	<0.001

Table 6: Parameters for the relation between ozone uptake (phytotoxic ozone dose, POD, mmol m^{-2}, with a threshold of 0 or 1 nmol m^{-2} s^{-1}, respectively) estimated using different uptake models in comparison to a direct calculation from sapflow (Figure 7, Figure 8) and average ratio between sapflow and model.

			Average ratio between model and sapflow		
model	parameter	R^2	estimate	95% confidence intervals	
envelope	POD0	0.807	0.66	0.57	0.74
multivariate	POD0	0.879	1.00	0.86	1.14
DO_3SE	POD0	0.818	1.10	0.92	1.27
envelope	POD1	0.781	0.63	0.52	0.75
multivariate	POD1	0.846	1.26	0.97	1.56
DO_3SE	POD1	0.761	1.39	0.99	1.79

Figure legends

Figure 1: Distribution of the optimum time lag in Hofstetten, Muri und Sagno. Units are days per tree (total of measurement days: Hofstetten 739, Muri 564 and Sagno 1033).

Figure 2: Relative conductance in relation to air temperature. Data points: normalized 90th percentile values per temperature class (2°C). Black line: nonlinear regression through the points of the envelope curve (for parameters see Table 4). Grey line: multivariate nonlinear regression (for parameters see Table 5).

Figure 3: Relative conductance in relation to vapour pressure deficit. Data points: 90th percentiles per VPD class (0.2 kPa) normalized to 1 at a VPD of 1 kPa. The black line is the fit to the data with the parameters listed in Table 4. Grey line: multivariate nonlinear regression (for parameters see Table 5).

Figure 4: Relative conductance in relation to photosynthetic active radiation. Data points: normalized 90th percentiles per PAR class (200 μmol m^{-2}, except for values <200 .μmol m^{-2} where a 100 μmol m^{-2} class width was chosen). The black line is the fit to the data with the parameters listed in Table 4. Grey line: multivariate nonlinear regression (for parameters see Table 5).

Figure 5: Relation between the canopy conductance and soil water potential. Data points: daily maximum values for the hours 7-10, averaged by soil water potential class and normalized to an intercept of 1 (dataset with MPa-values ≠ 0: n=380 for Muri and n=419 for Sagno).

Figure 6: Average measured (sapflow) or modelled conductance (envelope curve, multivariate, DO_3SE) in relation to VPD.

Figure 7: Phytotoxic ozone dose (flux cumulated for the periods with valid sap flow data within one season; mmol m^{-2}, POD0) for each tree estimated with the

parameters from different models (y-axis) in relation to ozone uptake calculated with conductances obtained directly from sap flow (x-axis). Left: envelope model (model 1), center: multivariate model (model 2), right: DO_3SE model. Black line: regression (with intercept), grey line: 1:1-line. For statistics see Table 6.

Figure 8: As Figure 7 but uptake calculated with a threshold of 1 nmol m^{-2} s^{-1} (POD1). For statistics see Table 6.

Figure 9: Difference between daily sums of ozone uptake estimated from sapflow and uptake modelled with the DO_3SE model (black, circles), the envelope model (dark grey, triangles) or with the multivariate model (light grey, squares) plotted against site and year (a), 24h-average of temperature (b), daily maximum of VPD (c), maximum photosynthetic active radiation (d), daily maximum of ozone (e) and measured soil water potential (f). Bars: 95% confidence intervals.

Figure 10: Relative conductance after budbreak (daily averages for the hours 11-14). Line: fit according to equation 8.

Figures

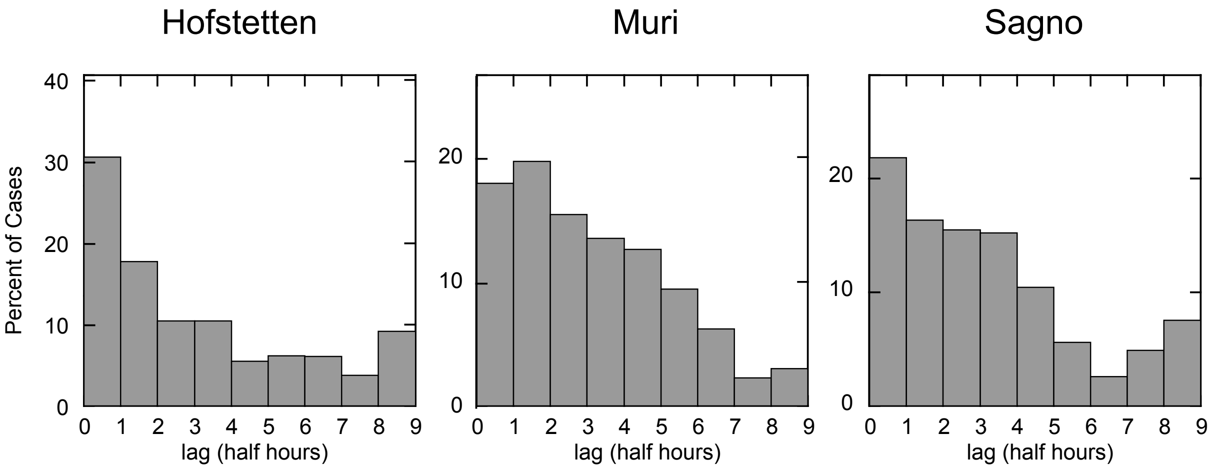

Figure 1

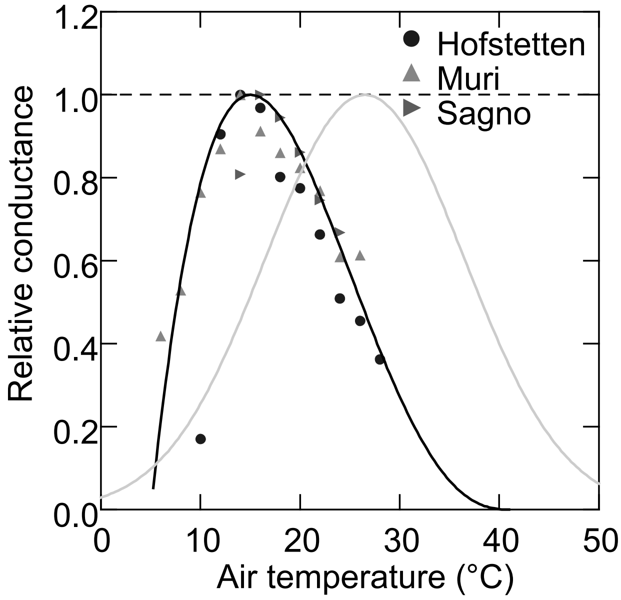

Figure 2

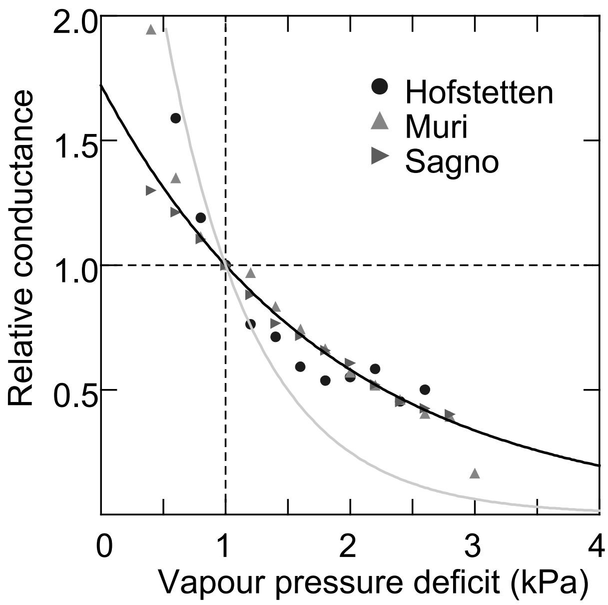

Figure 3

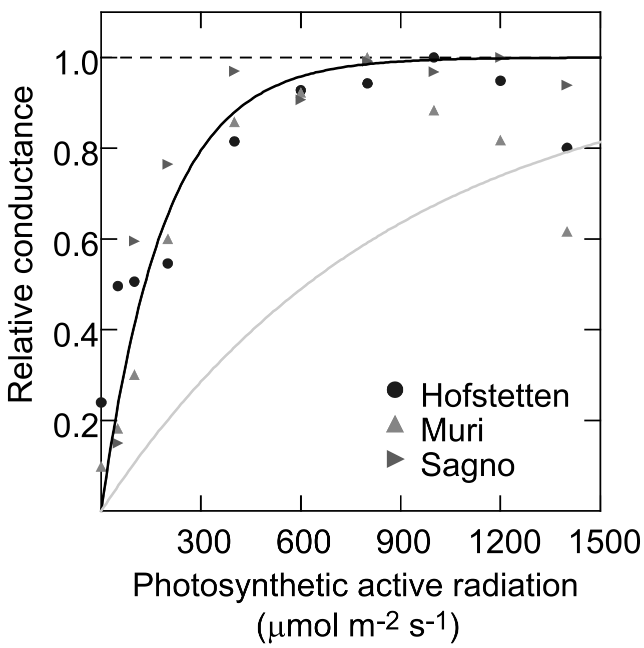

Figure 4

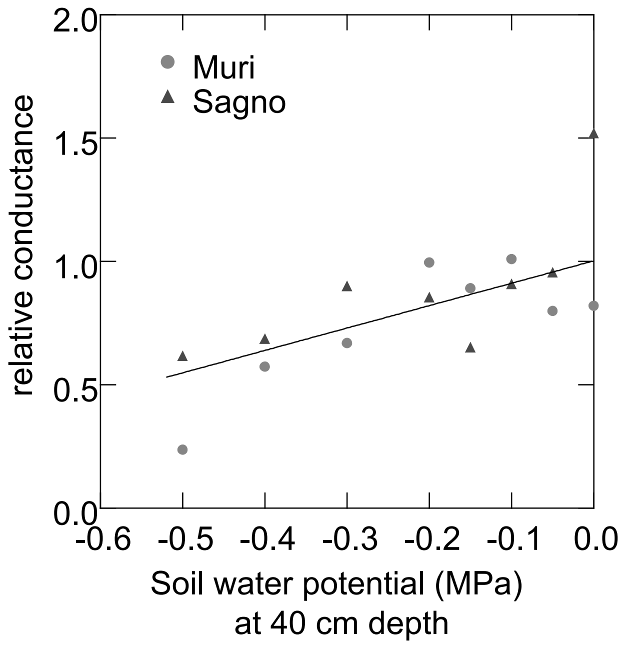

Figure 5

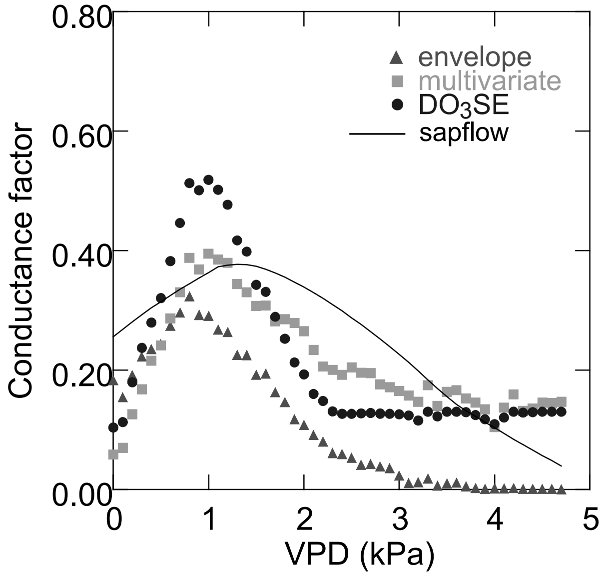

Figure 6

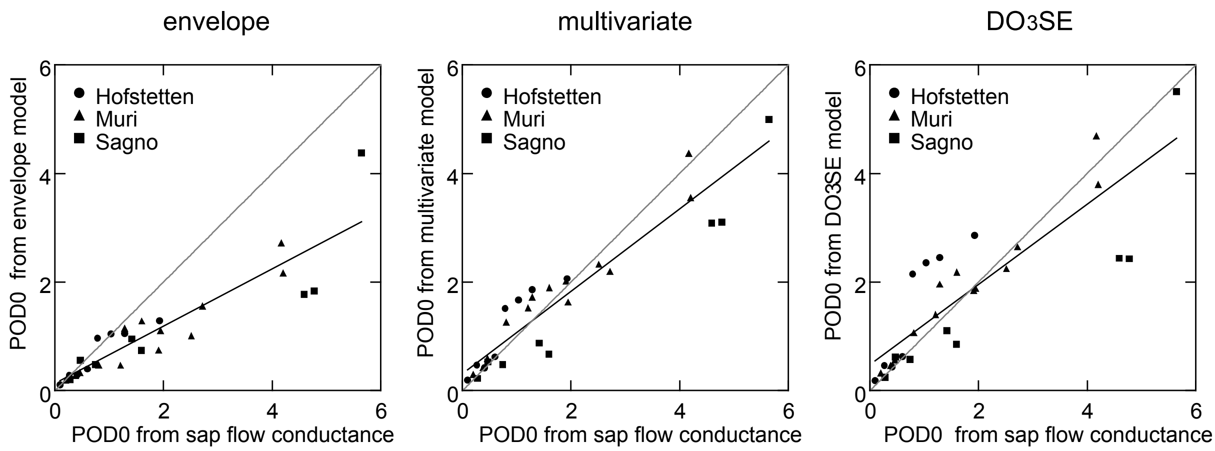

Figure 7

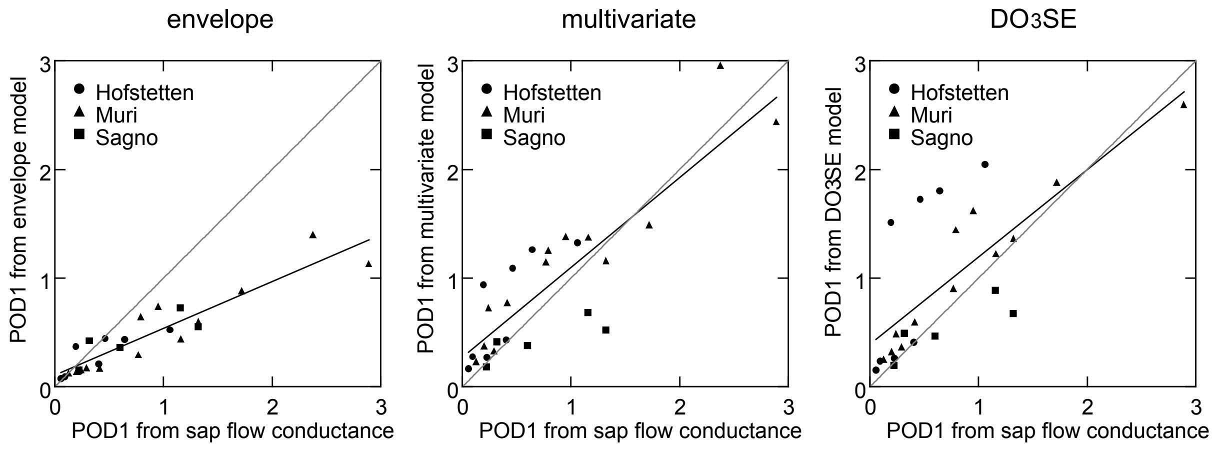

Figure 8

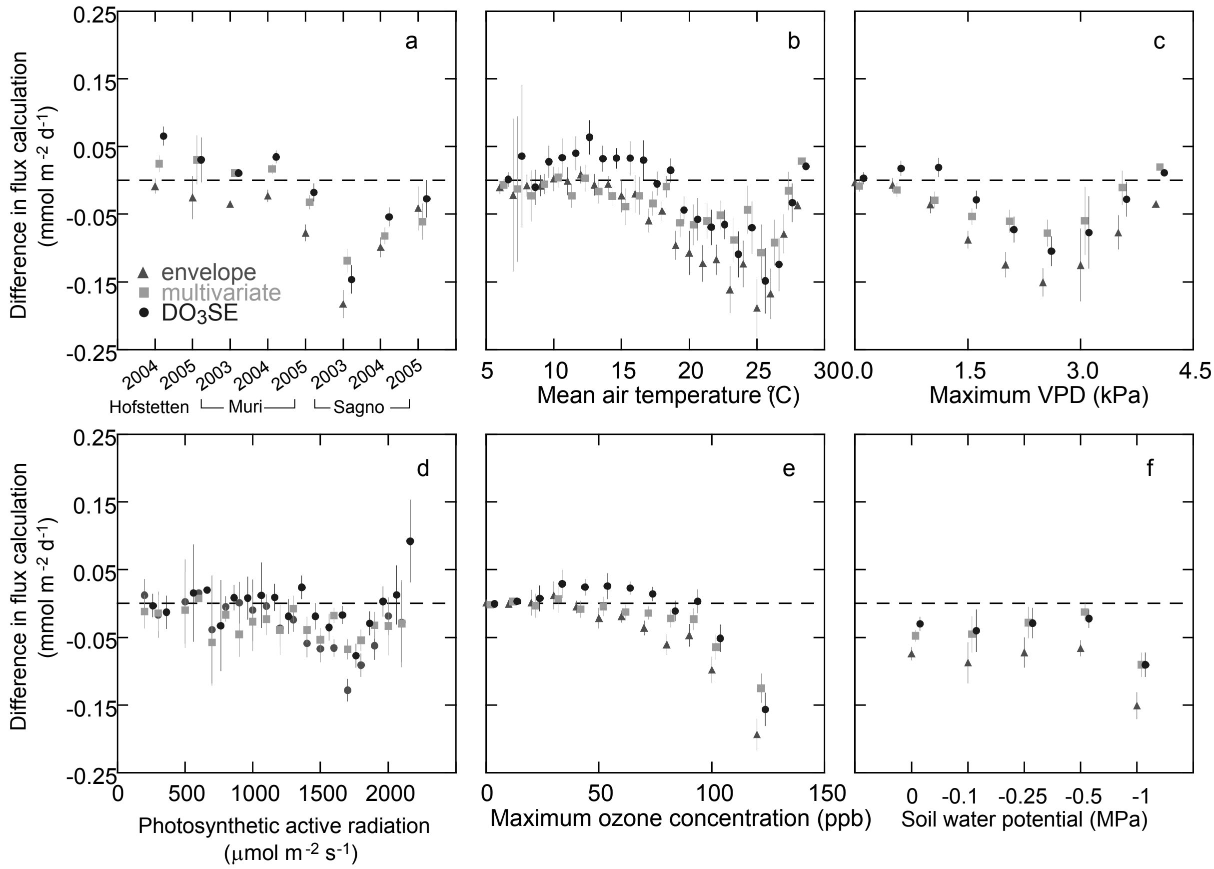

Figure 9

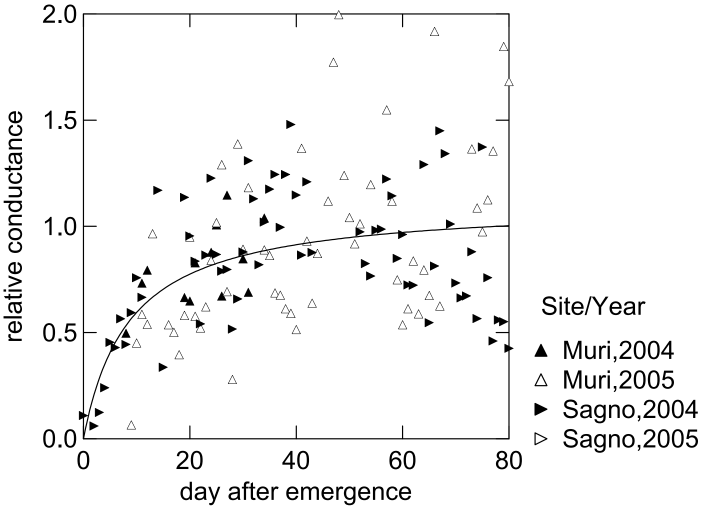
2.0
1.5
1.0
0.5
0.0
relative conductance
0
20
40
60
80
day after emergence
Site/Year
Muri,2004
Muri,2005
Sagno,2004
Sagno,2005

Figure 10